Adsorption and Photocatalytic Degradation of Eriochrome Black-T by TiO_2 of Different Shapes

A
Thesis Submitted
In partial fulfilment for the award of the degree of

MASTER OF SCIENCE
IN
CHEMISTRY

Submitted by
SANDEEP KAUR
Reg. No. 301102012

Under the supervision of
Dr. BONAMALI PAL
Associate Professor

SCHOOL OF CHEMISTRY AND BIOCHEMISTRY
THAPAR UNIVERSITY
PATIALA-147 004

JULY, 2013

CERTIFICATE

This is to certify that the project entitled "**Adsorption and Photocatalytic Degradation of Eriochrome Black-T by TiO_2 of Different Shapes**" being submitted by Sandeep Kaur, Roll No. 301102012 in partial fulfilment of the requirements for the award of degree of Master of Science, in School of Chemistry and Biochemistry, Thapar University, Patiala, is a bonifide work carried out under my supervision and guidance. The report has not been submitted for the award of any other degree or certificate in this or any other university.

Dr. Bonamali Pal
Associate Professor
School of Chemistry and Biochemistry
Thapar University, Patiala

Dr. Satham Singh
Associate Professor & Head
School of Chemistry and Biochemistry
Thapar University, Patiala

Dr. S.K Mohapatra
Dean Academic Affairs
Thapar University, Patiala

CANDIDATE'S DECLARATION

I hereby declare that the work which is being presented in the dissertation entitled "**Adsorption and Photocatalytic Degradation of Eriochrome Black-T by TiO_2 of Different Shapes**" in partial fulfilment of the requirements for the award of the degree of **Master of Science** in Chemistry, School of Chemistry and Biochemistry, Thapar University, Patiala is an authentic record of my own work during a period of six months from January 2013 to July 2013, under the supervision of Dr. Bonamali Pal, Associate Professor, School of Chemistry and Biochemistry, Thapar University, Patiala. I have not submitted the matter embodied in this thesis for the award of any other degree.

Sandeep Kaur

Place: Patiala

Sandeep Kaur

Date:

This is to certify that the above statement given by the candidate is correct and true to the best of our knowledge.

Dr. Bonamali Pal
Associate Professor & Supervisor
School of Chemistry and Biochemistry
Thapar University, Patiala

Dr. Satnam Singh
Associate Professor & Head
School of Chemistry and Biochemistry
Thapar University, Patiala

ACKNOWLEDGEMENT

I am thankful to **Dr. BONAMALI PAL,** Associate Professor, School of Chemistry and Biochemistry, Thapar University, Patiala, for his guidance and support.

Special thanks to **Rupinder Kaur, Rohit Singh, Nidhi Gupta and Inderpreet Singh Grover** for their kind cooperation during the project work.

Words fail me to express my thanks to my family/friends for their selfless sacrifice, encouragement and heart full blessings that continue to enlighten my life.

Sandeep Kaur

SANDEEP KAUR

Date:

Place: Patiala

Abstract

Titania based nanocatalysts of different morphologies having superior surface properties such as high surface area and pore volume are getting wide importance in adsorption and photocatalysis research for the degradation of textile dyes. Hence, present work demonstrates the influence of BET surface area, surface charge, pore volume and Fe^{+3} and Pt^{+4} ions impregnation onto as-prepared TiO_2 nanostructure for the dark adsorption and photocatalytic degradation of Eriochrome Black-T dye. Inspite of the least surface area of P25-TiO_2 among titania nanotubes and nanorods, highest dark adsorption for anionic Eriochrome black T has been found it, which can be accredited to its cationic surface responsible for better adsorption of oppositely charged dye molecules. Fe^{+3} and Pt^{+4} loading have been done to enhance the rate of adsorption and photocatalytic rate. Fe^{+3} loaded P25-TiO_2 is found to show the highest adsorption rate, 8.6×10^{-2} min^{-1} as compared to P25-TiO_2 , 8.06×10^{-2} min^{-1} followed by nanotubes, 2.0×10^{-2} min^{-1} and nanorods, 3.24×10^{-2} min^{-1}. The dark adsorption behaviour is investigated by varying the catalyst and dye concentration that follows the Freundlich adsorption isotherm with adsorption constant (K) varies from 4.0×10^{-2} – 5.4×10^{-2} μmol/ml and the value of n lies between 0.4–1, indicating pseudo-first order kinetic for the adsorption of present dye. Moreover, the photocatalytic degradation of dye also follows pseudo first-order decay kinetics. The k_{obs} values for photocatalytic degradation indicated an inverse dependence on the initial dye concentration and were fitted to the Langmuir-Hinshelwood equation. Photodegradation and adsorption rate increased with titania nanocatalysts dosage, but overdoses did not increase the photocatalytic efficiency. The photoinduced dissipation of Eriochrome Black-T results into formation of a number of intermediate photoproducts among them few has been identified by GC-MS analysis as: 2-diazenylnaphthalen-1-ol, 7-nitro-1,8a-dihydronaphthalene-1,3-diol,3-hydroxy-7-nitroso-1,8a-dihydronaphthalene-1sulfonoperoxoic acid, and 3-hydroxy-7-nitro-1,8a-dihydronaphthalene-1-carboxylic acid etc.

CONTENTS

1. Introduction

Textile waste water consists of dyes, pigments, pharmaceutical products, industrial chemicals and various organic compounds which are stable to light, oxidizing agent, and are resistant to aerobic digestion that posing a threat to the environment [1-4]. Estimates indicate that approximately 12% of synthetic textile dyes such as caramine, indigo red, Red 120, rhodamine B, methylene blue, Eriochrome black-T (EBT), etc. used each year [5,6] are lost during manufacture and processing operations, and 20% of these lost dyes enter the environment through effluents derived from the treatment of industrial wastewaters. Although conventional chemical and biological treatments [7-9] have been applied for the removal of dyes from textile waste water but these processes are insufficient in removing dye contaminants.

In this context, adsorption over biodegradable materials has evolved into one of the most effective physical process for the decolorization of textile waste waters, and is economically feasible [10,11]. The most commonly used adsorbent for color removal is activated carbon, because of its capability for efficiently adsorbing a broad range of different types of adsorbates. Due to high cost of activated carbon, the use of alternative adsorbents is attractive [12-16] such as hen feathers, rice husk; neem saw dust, banana peels, clays, deoiled soya, coir pith, etc. as important constituents of many natural systems with lower costs. For example, EBT was adsorbed over the surface of eucalyptus bark, methylene blue and EBT has been removed from aqueous solution by biosorption using scolymus hispanicus, methylene blue was adsorbed on silt fractioned from bijoypur soil, Bangladesh, etc [15-17]. This adsorption phenomemenon leads to the removal of dyes onto the adsorbent surface only that finally dumped into the land which again pollutes the air and soil and causes serious environmental damage. Therefore, the complete mineralization or detoxification of dye to environmental benign CO_2 , H_2O, nitrates, etc. is one of the challenging research topics [18].

Nowadays, photocatalysis using titanium dioxide (TiO_2) semiconductor has been found to be a greener approach for the degradation of harmful dye pollutants compounds completely [19,20]. Titanium dioxide is a widely accepted photocatalyst due to its high oxidation efficiency, non-toxicity, high photostability, chemical inertness and

environmentally friendly nature [21-23]. TiO_2 semiconductor with a wide band gap of ~ 3.2 eV mineralizes a large range of refractory organic pollutants such as herbicides, dyes, pesticides, phenolic compounds, tetracycline, sulfamethazine, etc [24] under UV irradiation. Such photocatalytic processes is explained as when a photon with energy equal to or greater than the TiO_2 energy gap (3.2 eV) is absorbed by a TiO_2 particle, hole (h^+) is created in the valence band and electrons (e^-) in the conductivity band which diffuses to the surface of titania and takes part in oxidation-reduction reactions of the adsorbed susbstrates. The hole can also react with water to produce hydroxyl radicals and the electron can reduce O_2 to produce strongly oxidizing superoxide ions and hydroxyl radicals [25-28] (scheme 1). Therefore, both reduction and oxidation by e^- and h^+ can be utilized for the conversion of organic substrates under deaerated conditions.

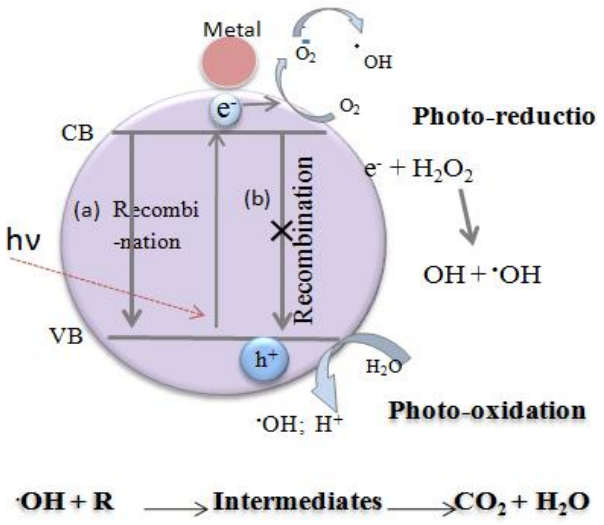

Scheme 1. Mechanism for the TiO_2 mediated photodegradation of pollutants.

For example, Singhal et al. [29] studied the photocatalytic degradation of cetylpyridinium over TiO_2 powders. Photocatalytic decomposition of organophosphates in irradiated TiO_2 has been carried out by Shea and co-workers [30]. Hyoung et al. [31] studied the photocatalytic degradation of reactive Red 120 dye using TiO_2 particles as photocatalyst under UV irradiation. Study of photocatalytic degradation of Indigo Caramine in aqueous suspension has been carried out using nanosized TiO_2 particles by varying catalyst dose, dye concentration, pH and contact time (park and Shrivastava) [32,33]. Ong et al. [34] studied the photodegaradation of congo red and reactive yellow 2 using immobilized TiO_2. Serpone and Pelizzetti [35] have reported that TiO_2 and ZnO are the two most active catalysts in the degradation of pentachlorophenol.

Furthermore, metal loading is also done to improve the photocatalytic activity of semiconductors to a high extent. Metallization of TiO_2 surface with noble metals such as

Fe, Cu, Au, Ag or Pt has been investigated from the early times of photocatalysis to increase the photocatalytic activity by preventing the e^{-}-h^{+} recombination [36-38] (scheme 1). The metal ion or metal doped semiconductor composites exhibit shifts in the Fermi level to more negative potentials and hence enhanced the photocatalytic rate. The CB and VB positions of TiO_2 crystallites are also known to vary depending on the size and shape of particle and thereby alter the TiO_2 photoactivity [39]. Therefore, different TiO_2 shapes and other titania based composite nanostructures have attracted a great deal of research interest due to their surface structural, and morphological advantages. For example, lengthy titania nanorods, and nanotube exhibit high photocatalytic activity relative to P25-TiO_2 particles due to better delocalization of excited e^{-}/h+ pairs and well developed space charge region that reduced the recombination time of photogenerated charge species [40]. Hence, recently titania nanotubes and titania nanorod morphologies displays flexible photoactivity depending on their crystal phase composition, geometric morphology and surface area. We examine the effect of various morphologies of titania nanostructures (spheres, rods and tubes) and Fe^{+3} and Pt^{+4} loading onto these different shapes for the adsorption and photocatalytic degradation of EBT.

2. Research gap and Objectives

Although, extensive research has been done on the adsorption of a variety of dyes using various adsorbents, yet few reports exist for the degradation of EBT using TiO_2. EBT cause irritation to the eyes, skin and respiratory tract system. EBT (molecular structure-Scheme 2) is used as an indicator in compexometric titrations for estimation of $Ca^{2+,}$ Mg^{2+} and Zn^{2+} ions and for biological staining. It is used for dyeing silk, wool, nylon, multifibres after pretreatment with chromium salts which is harmful for the human kind. It is worthy to mention here that most of the dyes were degraded using mostly active P25-TiO_2 nanosphers, however, the influence of geometric shape and surface area, surface charge, pore volume of adsorbent, etc., has not been studied in detail yet. The influence of Fe^{+3} and Pt^{+4} impregnation on the various shapes of TiO_2 with different

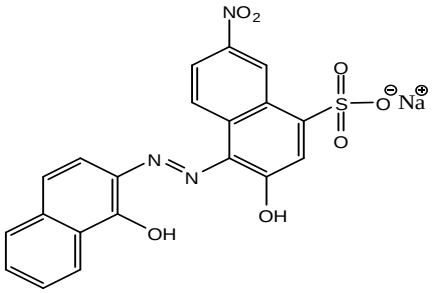

Scheme 2. Molecular structure of Eriochrome Black-T.

surface structures are studied for the adsorption and rapid decomposition of EBT dye by photocatalysis technique and following objectives are proposed.

Objectives

- To study the adsorption efficiency and photocatalytic degradation of Eriochrome black-T dye over as-prepared TiO_2 nanorods and nanotubes as compared to mostly studied P25-TiO_2 catalyst as a function of their surface area and geometric morphology.
- To improve the photocatalytic activity for the EBT degradation by Fe^{+3} and Pt^{+4} impregnated TiO_2 nanostructures.

3. Experimental

3.1. Material and methods

Ferric nitrate ($Fe(NO_3)_3.3H_2O$), hexachloroplatinate ($H_2PtCl_6.xH_2O$), sodium sulphate anhydrous (Na_2SO_4), methanol (CH_3OH), ethyl acetate ($CH_3COOC_2H_5$) and Eriochrome black-T ($C_{20}H_{12}N_3O_7SNa$) were purchased from Loba Chemie, India. N_2 (99.999%) gas was obtained from BOC India Ltd. Commercially available P25-TiO_2 was obtained from Degussa Corporation Germany.

3.2. Synthesis of various titania nanostructures

Titania nanotubes (nanotubes) and titania nanorods (nanorod) were synthesized in our laboratory [41] as per following method. Commercially available P25-TiO_2 was used as a precursor for nanotubes, which was prepared by autoclaving the P25-TiO_2 (4.73 g) with 72 ml of NaOH (10 M) in a teflon lined autoclave (capacity 80 ml) at 120 ^oC for 20 h. The slurry thus obtained was washed repeatedly with 0.1N HNO_3, water and methanol. Nanorods were synthesized from nanotubes by keeping aqueous slurry of nanotubes (3.2 g in 64 ml, pH = 5.6) in autoclave at 175 $^\circ C$ for 48 h. After the hydrothermal treatment, the resulted slurry was filtered, washed with distilled water and methanol, and dried at 70 ^oC for 3 h.

3.3. Metal (Fe^{+3} and Pt^{+4}) impregnation onto TiO_2 nanostructures

Metal loaded titania nanocrystals (P25-TiO_2, nanotubes and nanorods) were synthesized through metal impregnation method [42] using aqueous solution of metal salts (ferric nitrate, 0.01M and hexachloroplatinate, 0.01M). In a typical experiment, 500 mg of titania

nanocrystals were individually mixed with 50 ml distilled water by adding requisite amounts (1 wt%) of metal salts solution, stirred for 6 h, afterwards dried at 100 $^{\circ}$C with stirring, grinded and then used for dark adsorption and photocatalytic studies. Samples thus obtained are abbreviated as: Fe^{+3}-P25-TiO_2 (Fe^{+3} impregnated P25-TiO_2), Fe^{+3}-I-nanotubes (Fe^{+3} impregnated nanotubes), Fe^{+3}-I-nanorod (Fe^{+3} impregnated nanorod), Pt^{+4}-P25-TiO_2 (Pt^{+4} impregnated P25-TiO_2), Pt^{+4}-I-nanotubes (Pt^{+4} impregnated nanotubes) and Pt^{+4}-I-nanorods (Pt^{+4} impregnated nanorods).

3.4. Dark adsorption studies

The adsorption studies were performed using aqueous solutions of dyes. For this purpose 5 ml dye solution of different concentrations (0.01-0.35 mM) were magnetically stirred separately in presence of bare and metal impregnated catalysts (5-30 mg) in dark up to 120 min. Thereafter, the suspensions were collected after regular time intervals (20 min) filtered through cellulose filter (0.22 μm) and then analyzed by UV-vis spectrophotometer at λ_{max} = 612 nm for EBT dye.

3.5. Photocatalytic activity study

The comparative photocatalytic activity of various bare and metal impregnated titania nanocrystals were assessed by taking 5 to 30 mg catalysts, 5 ml (0.01-0.35 mM) aqueous solution of EBT into a beaker under UV light (125 W Hg arc, 10.4 mW/cm^2) irradiation for 120 min. After that, the samples were collected at regular time intervals (20 min) filtered through cellulose filter (0.22 μm) and then analyzed by UV-Visible spectroscope (λ_{max} = 612 nm).

3.6. GC-MS analysis

In a typical experiment 5 ml of EBT solution after 120 min of UV-light exposure was collected, centrifuged (5000-8000 rpm), filtered through cellulose filter (0.22 μm) and then extracted with three successive quantities (5 ml) of ethyl acteate. The sample (ethyl acetate) thus obtained was passes through sodium sulphate (anhyd.), evaporated to dryness over rota-evaporator, and its traces removed over gentle stream of N_2 gas. Residue thus obtained was redissolve in methanol (GC grade) and analyzed by Gas chromatography-Mass spectroscope (Shimadzu, GC-2010 and GC-MS-QP 2010 plus) using RTX-5Sil-MS column (30 m × 0.25 mm × 0.25 μm). Helium was used as a carrier gas with a flow of 1ml/min through capillary column. Injector was maintained at 240 $^{\circ}$C, while transfer line

was kept at 260 °C and 1 µl of the sample was injected. Oven was programmed at 60 °C to 300 °C @ 6 °C/min rise of temperature.

3.7. Characterization techniques

All the samples were characterized by XRD (Panalytical Xpert using Cu Kα = 1.54178A°), and TEM-107 (Hitachi 7500, 2A° , 120 KV) for size-shape analysis. BET surface area and pore volume were measured with (Smart Sorb 93) using 150 mg of sample, preheated at 150 °C for 1 h using calibration gases (for surface area N_2:He::70:30 and N_2:He::30:70 for pore volume) at cryogenic temperature. Surface charge density (Mutek-PCD03pH) analysis was carried out using 50 ml aqueous slurry (0.6 mg/ml) of different titania nanocrystals as reported in our laboratory.

4. Results and Discussion

4.1. X-ray diffraction analysis

The XRD pattern of as-prepared nanotube and nanorod in comparison to P25-TiO_2 are shown in figure 1. The as-prepared nanotube found to possess orthorhombic crystal structure for $Na_2Ti_2O_5 \cdot H_2O$ as confirmed by its characteristic peak at 2θ = 24.05° and is in agreement with our previous report [41]. Whereas, the nanorod prepared form nanotubes through hydrothermal route is found to be of pure anatase phase as evidenced by its characteristic peak at 2θ = 25.3°. The hydrothermal treatment of nanotubes at 175 °C for 48 h under mild acidic conditions favors the growth of anatase nanorod. It was proposed that during hydrothermal treatment the nanotube structure got ruptured dissolved and rearranged to form anatase nanocrystals that would join in a way known as "*oriented attachment*" to form nanorod morphology. The nanorod particles show intense diffraction lines (Fig. 1) indicating high crystallinity of nanorod,

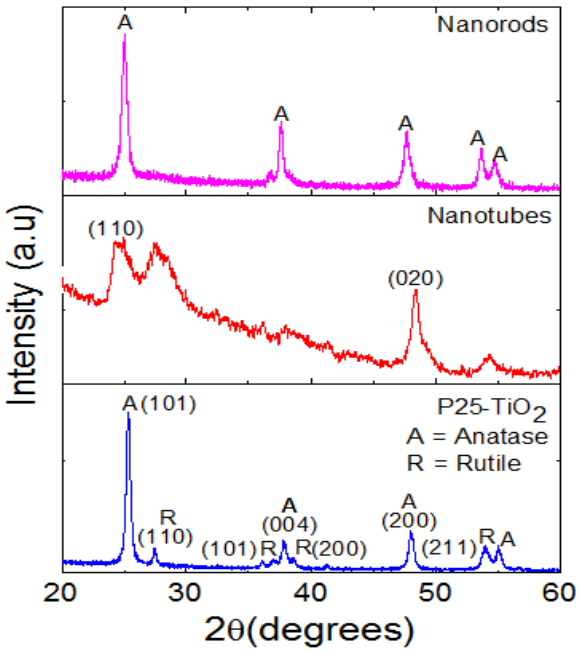

Figure 1. XRD patterns of various titania catalysts.

despite being synthesized at 175 ^{o}C autoclaving as compared to amorphous nature of nanotube that exhibits broad XRD peaks.

4.2. TEM analysis

Transmission electron microscope (TEM) has been used to investigate the dissimilarities in the morphologies of various bare (Fig. 2) and metal impregnated (Fig. 3) catalysts. TEM image for P25-TiO_2 (Fig. 2a) clearly reveals that it is a mixture of non-spherical shaped nanoparticles.

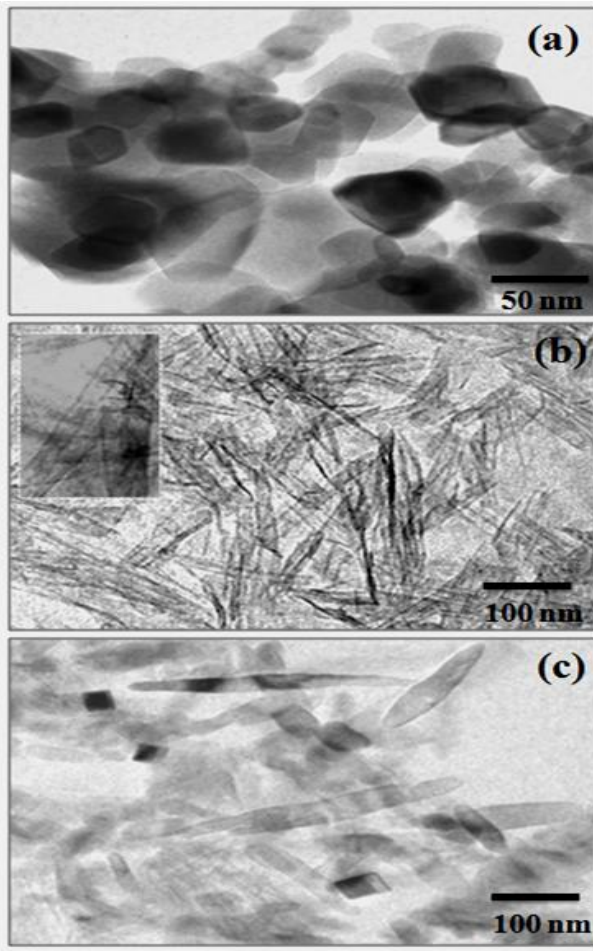

Figure 2. TEM images of bare (a) P25-TiO_2, (b) titania nanotube and (c) nanorod: inset (b) hollow interior of nanotube.

Whereas, nanotubes (Fig. 2b) found to possess straw like open ended morphology with hollow interior (inset Fig. 2b), having diameter 9–12 nm and length 82–115 nm. On the other hand, the TEM image (Fig. 2c) depicts the formation of lengthy nanorod particles of various dimensions after hydrothermal treatment of nanotubes for 48 h in acidic media

(pH= 5.6). There are some long and short rice like morphology of nanorod particles having diameter 8–13 nm and length 81–134 nm are seen in figure 2c.

Figure 3 represents the TEM images after impregnation of 1 wt% Fe^{+3} and Pt^{+4} onto P25-TiO_2 and nanotube. It is clearly visualize that impregnation of Fe^{+3} (Fig. 3a and 3b) and

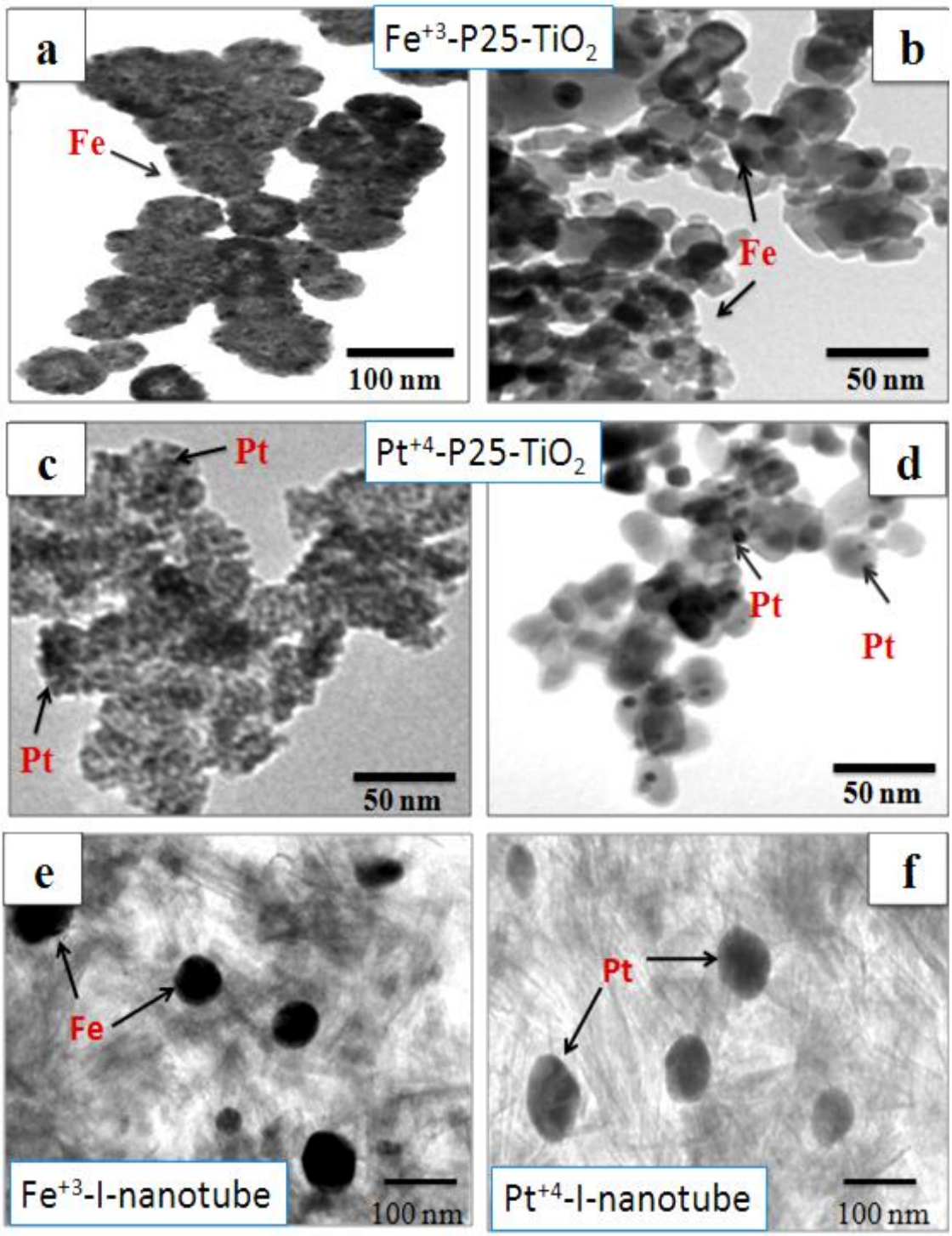

Figure 3. TEM images of Fe^{+3} and Pt^{+4} impregnated TiO_2 catalysts

Pt^{+4} (Fig. 3c and 3d) onto P25-TiO_2 results into deposition of these metals in spherical shape, which is homogeneous with very narrow particles size distribution ca. 4-8 nm. In contrast to this, the non uniform repartition of the Fe^{+3} and Pt^{+4} with a their respective particles size of 30-35 nm and 40-45 nm, onto nanotube has been found (Fig. 3e and 3f). This might be arises from the step of incipient wetness impregnation itself, since there is no specific interaction between these metal ions and the support.

4.3. BET Surface area and pore volume analysis

The BET surface area (S_{BET}) of as-prepared nanotube, nanorod and P25-TiO_2 particles is found to be 176, 79 and 56 m^2g^{-1}, respectively, are in accordance with their structural morphology. Although, the dimensions of nanotubes and nanorod are same, yet the surface area of the former was around 2.2 times higher than the later one, ascribed to its hollow and open ended morphology as observed clearly in TEM images (Fig. 2b and 2c).

The decrease in S_{BET} of nanorod suggests that the hollow nanotube has collapsed and compacted to solid and rigid nanorod rice like particles during autoclaving at 175 ^oC for 48 h. It was found that S_{BET} is decreased after 1 wt% Fe^{+3} and Pt^{+4} impregnation onto studied nanoparticles of different shapes as can be seen in table 1. This decrement in S_{BET} can be accounted for the partial surface coverage of TNP particles surface by the metal nanodeposits as evidenced by TEM images (Fig. 3e-3f). It is interesting to notice that the decrease of S_{BET} due to Pt^{+4} and Fe^{+3} impregnation over nanotube is always higher than Pt^{+4}/Fe^{+3} loaded P25-TiO_2 and nanorod particles despite having same amount (1 wt%) metal impregnation. This probably occurs due to blockage of the hollow porous surface and open outlet channel in a little extent, though we have no such proof to confirm the same. Moreover, the difference in S_{BET} among the Pt^{+4} and Fe^{+3} impregnated titanaia nanocrystals is due to the difference in their adsorption capacity of the gases (N_2:He::70:30) during BET analysis. These bare and metal loaded nanocrystals have been evaluated for their respective pore volumes, as it provides insight into porosity of the material, which is necessary for the adsorption of the substrate. It found that pore volume of nanotubes is around 3.3 times more in comparison to nanorod and P25-TiO_2 (Table 1) indicating its highly porous structure. However, impregnation of Pt^{+4} and Fe^{+3} diminishes the pore volume (Table 1) of titania nanocrystals, ascribed to the occupancy of the available pores by these metal ions, resulted into decrement of pore volume.

Table 1 : Physicochemical parameters of bare and metal impregnated titania nanostructures of different shapes

S.No	Titania Catalysts	Phase	Size (nm)	Surface Area (m^2/g)	Surface Charge (μequi./g)	Pore Volume (cc/g)
1	P25-TiO_2	Anatase:Rutile	30-50	56	+8.82	0.05
2	Nanotubes	Orthorhombic	L =82-115 D = 9-12	176	-1.79	0.09
3	Nanorod	Anatase	L =81-134 D = 8-13	79	-6.17	0.3
4	Fe^{+3}-P25-TiO_2	Anatase:Rutile	--	48	+10. 27	0.009
5	Pt^{+4}-P25-TiO_2	Anatase:Rutile	--	36	--	0.005
6	Fe^{+3}-I-nanotubes	Anatase	--	164	--	--
7	Pt^{+4}- I-nanotubes	Anatase	--	146	--	--
8	Fe^{+3}-I-nanorods	Anatase	--	70	--	--
9	Pt^{+4}- I-nanorods	Anatase	--	59	--	--

4.4. Dark adsorption of EBT on various shapes of TiO_2 catalysts

4.4.1. Effect of TiO_2 concentration

Various titania nanostuures and Fe^{+3}-P25-TiO_2 have been used for evaluating the comparative adsorption of EBT (0.25 mM). Initially, a series of experiments were conducted to find an optimum catalyst concentration by varying the concentration of TiO_2 (5-30 mg) of different shapes. It can be seen in figure 4 that on increasing the amount of TiO_2 (5-30 mg) catalyst, adsorption rate of EBT was highly enhanced. The EBT adsorption was found to be higher during first 20-30 min in all the cases. Results illustrated in figure 4 showed that initially the adsorption rate linearly increases (~75-95 %) and thereby

undergoes an exponential decrease as $C = C_0e^{-kt}$ in EBT concentration (0.25 mM) with increasing TiO_2 dosage upto 20 mg like conventional adsorption isotherm and further increasing TiO_2 (25-30 mg), the adsorption rate remained almost constant.

The observed enhancement in this range (5-20 mg) is probably due to an increased number of available adsorption sites on TiO_2 with rise in number of molecules ($3.77 \times 10^{19} - 1.51 \times$

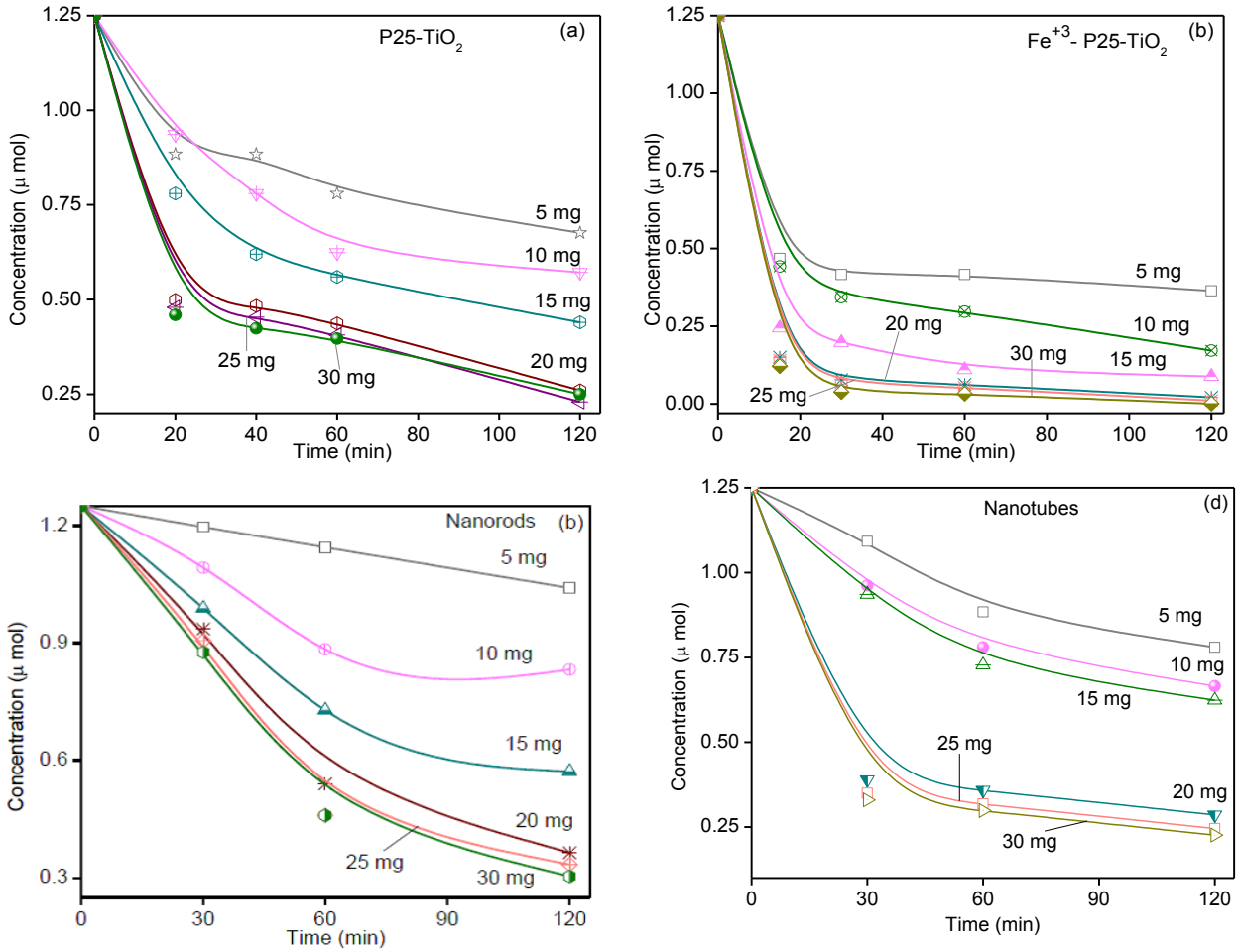

Figure 4. Time course of dark adsorption of Eriochrome black T (0.25 mM) with amount of different TiO_2 (a) P25-TiO_2 (b) Fe^{+3}-P25-TiO_2 (c) nanorods and (d) nanotubes.

10^{20}). On further addition of TiO_2 (30 mg = 2.26×10^{20} molecules), an increase in the surface layers of the TiO_2 particles does not further improve the adsorption rate because denser TiO_2 suspension become saturated with EBT. Hence, 20 mg of TiO_2 catalyst (1.51×10^{20} molecules of TiO_2) was used for the optimum adsorption for 0.25 mM aqueous EBT (576 mg) solution in all experiments for EBT degradation.

Among the various titania nanostructures, Fe^{+3}-P25-TiO_2 is found to showed the highest adsorption rate (8.6×10^{-2} µmol/mg/min^{-1}) as compared to P25-TiO_2 (8.06×10^{-2}) followed by nanotubes (2.0×10^{-2}) and nanorods (3.24×10^{-2}) as can be seen in scheme- 3a and 3b. The highest adsorption rate for Fe^{+3}-P25-TiO_2 has been ascribed to its highest surface charge (+10.0 µequi./g) due to presence of extra Fe^{+3} ions despite of its lower surface area (40 m^2/g) as compared to nanotubes that possesses highest surface area (176 m^2/g, table 1), because of the anionic nature of EBT dye. Thus, the attractive and repulsive interactions among the EBT molecules and catalyst are responsible for the dissimilar adsorption behavior in all catalysts. Since, P25-TiO_2 is positively charged as a result the attractive interaction exists between them that cause highest adsorption of EBT dye (Scheme-3a). Whereas, the repulsive interactions are present in between EBT and negatively changed nanotubes (-1.79 µequi.g^{-1}) and nanorods (-6.17 µequi./g) that renders its adsorption.

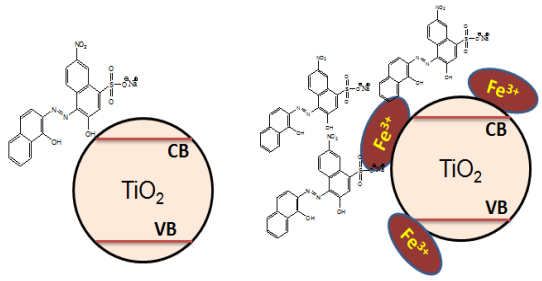

(a) **(b)**

Scheme 3. Effect of surface charge of bare and Fe^{+3} loaded TiO_2 on the EBT adsorption.

4.4.2. Dark adsorption isotherm

Generally, heterogeneous catalysts follow the Langmuir and Freundlich adsorption isotherms. These isotherms support the heterogeneity of the surface and assume that the adsorption occurs at sites with different energy of adsorption. The energy of adsorption varies as a function of surface coverage. Freundlich equation is applicable for multilayer adsorption and is mathematically expressed as:

$$\mathbf{x/m = Kc^{1/n} \quad or \ log\ x/m = log\ K + 1/n\ log\ C}$$

Where x = mass of adsorbate, m = mass of adsorbent, c = equilibrium concentration of adsorbate in solution. K and n are constants for a given adsorbate and adsorbent at a particular temperature. At high concentration, 1/n = 0, hence extent of adsorption becomes independent of concentration and follow zero order reaction kinetics. The adsorbed amount of dye was calculated by measuring the concentration of dye in solution before and after

adsorption using Freundlich isotherm equations. Fig. 5a shows the plot of adsorption constant at various TiO_2 concentrations (1 mg/ml– 6 mg/ml) for all TiO_2 morphologies.

Fig. 5b describes the extent of adsorption (x/m) as a function of catalyst concentration (1 mg/ml– 6 mg/ml) on TiO_2 nanostructures. It has been seen that the rate of adsorption and x/m first increases linearly and follow first order adsorption kinetics. But after a certain limit (~4 mg/ml), rates do not vary and become constant, follows zero order adsorption kinetics similar to Freundlich adsorption isotherm.

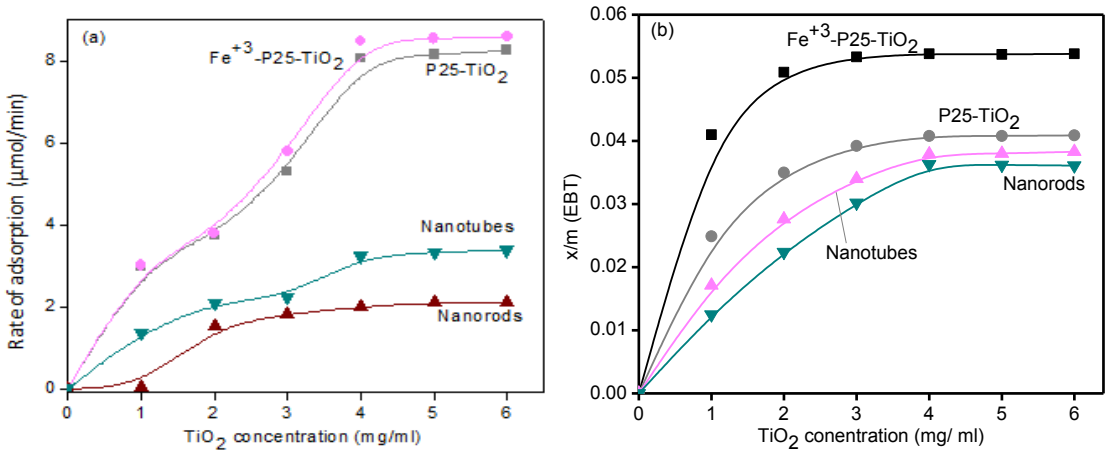

Figure 5. Variation of (a) adsorption constant and (b) Freundlich adsorption as a function of TiO_2 shapes and their concentration (1-6 mg/ml).

4.4.3. Effect of dye concentration

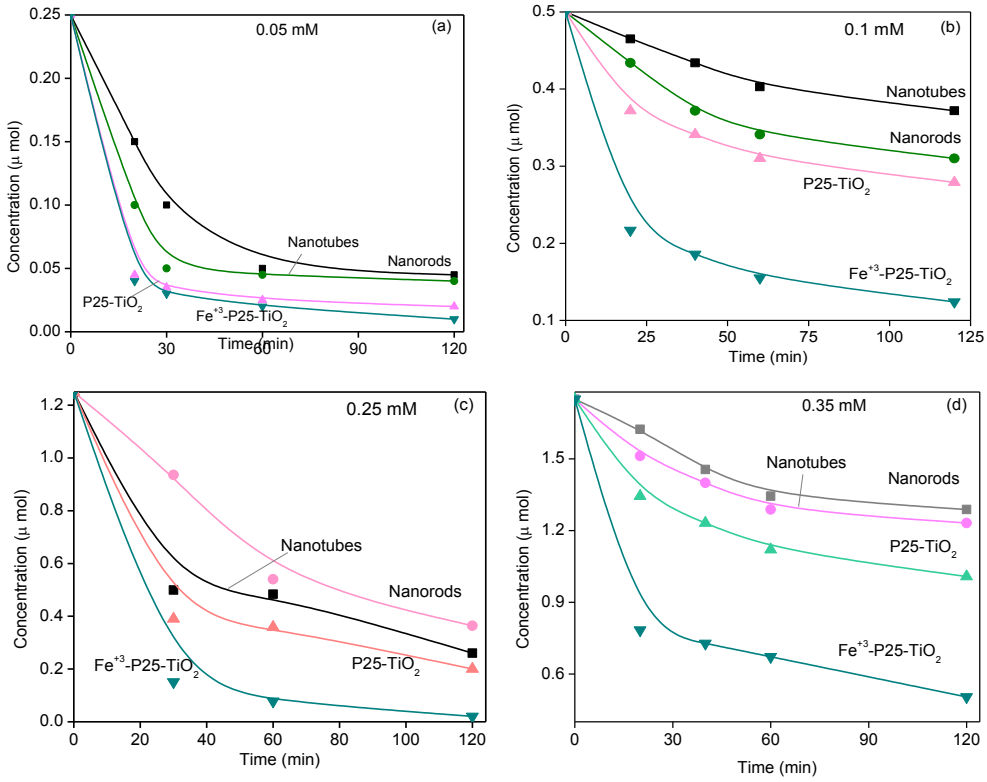

Figure 6. Time course of dark adsorption as a function of Eriochrome black-T concentration (0.01 mM – 0.35 mM) with different TiO_2 nanostructures.

The effect of the EBT concentration has been studied in a range between 0.01 mM to 0.35 mM for a constant TiO_2 dosage (4 mg/ml) as shown in figure 6. It is apparent from the data that adsorption decreases (~40 %) with increase in the concentration of dye (0.05-0.35 mM). This decrease might be due to the repulsive interactions among the anionic EBT dye molecules that become more pronounced with increase in its concentration. Subsequently, the attractive interactions between catalyst surface (P25-TiO_2 and Fe^{+3}-P25-TiO_2) become less that causes decrease in its adsorption. The Freundlich adsorption isotherm was also used here to study the extent of adsorption on to various shapes of TiO_2. The calculated log K value is found to be highest for the Fe^{+3}-P25-TiO_2 followed by P25-TiO_2 > nanotubes > and lowest for nanorods as seen in figure 7.

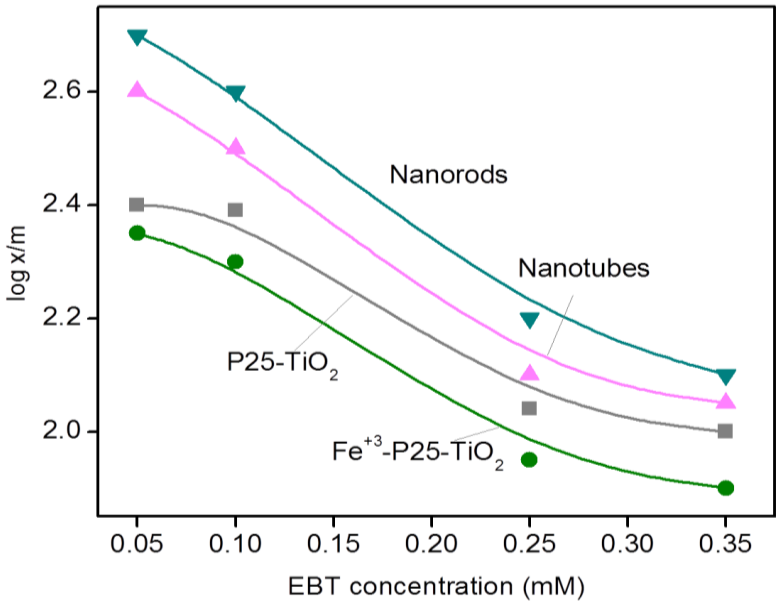

Figure 7. Effect of EBT concentration on the adsorption rate as a function of TiO_2 morphology.

4.5. Photocatalytic degradation of EBT dye

4.5.1. Effect of TiO_2 concentration on photodegradation rate

Figure 8 shows the influence of TiO_2 concentration (P25-TiO_2, ca. 1-6 mg/ml) on the degradation kinetics of EBT (0.25 mM) under UV irradiation for 2 h. Photodegradation of EBT enhances rapidly with increasing the amount of catalyst as observed in figure 8a because the number of active sites on the TiO_2 surface increases the number of hydroxal

and superoxide radicals that help in improving the photodegradation rate. It has been observed that 4 mg/ml of TiO_2 was the optimum dose for efficient degradation of dye as further addition does not improve much the photooxidation rate. Figure 8b clearly reveals the dependence of photooxidation rate on the TiO_2 concentration upto 4 mg/ml and thereby EBT photodegradation rate becomes almost constant on further increasing the amount of catalyst beyond 4 mg/ml. Thus optimum amount of TiO_2 dosage (4 mg/ml = 20 mg per 5 ml aqueous EBT dye solution is used for efficient photodegradation.

4.5.2. Effect of EBT concentration on photodegradation rate

4.5.2.1. Langmuir-Hinshelwood Equation

Literature explains that Langmuir-Hinshelwood expression has been successfully used to describe the dependence of the reaction rate on the initial concentration of the organic substrate for heterogeneous photocatalytic degradation. The Langmuir-Hinshelwood expression has been successfully used to describe the dependence of the reaction rate r_{EBT} on the initial concentration of the dye substrate $[EBT]_o$ for heterogeneous photocatalytic degradation:

$$r_{EBT} = -\frac{d[EBT]}{dt} = k_{obs}[EBT] = \frac{kK_{EBT}[EBT]}{1+K_{EBT}[EBT]_o}$$

Where K_{EBT} is the Langmuir-Hinshelwood adsorption equilibrium constant of Eriochrome black-T and k is the rate constant at the surface reaction. A plot of $1/k_{obs}$ vs. initial eriochrome concentration [EBT] gave a straight line (Fig. 9) indicating that the kinetics fit with a Langmuir- Hinshelwood equation and is given below:

$$\frac{1}{k_{obs}} = \frac{1}{kK_{EBT}} + \frac{[EBT]_o}{k}$$

Where k and K_{EBT} can be calculated from the intercept and slope.

The photocatalytic degradation of EBT has been investigated in aqueous suspension of TiO_2 at various EBT concentrations (0.05 mM to 0.35 mM). The experiment was carried out at constant catalyst dose ~25 mg. It was found that

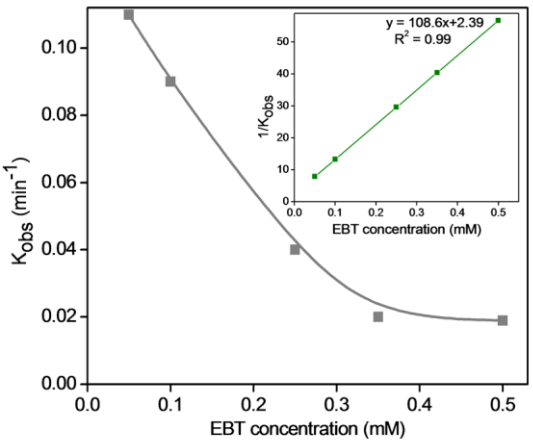

Figure 9. Effect of initial EBT concentration on the pseudo-first-order rate constant.

photocatalytic degradation rate decreases on increasing EBT concentration and observed that 0.25 mM of dye concentration was the optimum concentration for efficient degradation of EBT as shown in figure 9. A good correlation is obtained from the plot $1/k_{obs}$ vs. initial EBT concentration $[EBT]_o$ indicates (inset-Fig. 9) that the photocatalytic degradation of EBT occurred mainly at the TiO_2 surface and k and K_{EBT} obtained from the intercept and slope are found to be $0.19\ min^{-1}$ and 0.21 ml/mg, respectively.

Because for a fixed concentration of active sites remaining the same, the number of substrates ions accommodated in the interlayer space increases so that the degradation decreases. This may be due to the fact that with increase in initial concentration of the dye, more dye molecules are also adsorbed on the surface of TiO_2. Thus, increase in the number of substrate ions accommodating in inter layer spacing inhibit the action of catalyst which thereby decreases the reactive hydoral and superoxide free radicals attacking the dye molecules and photodegradation efficiency.

4.5.3. Influence of Fe^{+3} and Pt^{+4} impregnation into TiO_2 for EBT photodegradation

The presence of a metal ion on semiconductor nanoparticles is beneficial for maximizing the efficiency of photocatalytic reactions by preventing the e^--h^+ pair recombination as shown in scheme 1. Metal facilitates charge separation and promotes interfacial electron transfer at the interface by transferring electrons from the excited TiO_2 to metal until the two systems attain Fermi level equilibration. The difference in photocatalytic efficiency dependent on the nature, charge of the metal ion and shape of the catalyst is observed.

Figure 10a illustrates the effect of catalyst shape on the degradation of eriochrome black T. Comparative effect on metal loading on the various shapes of TiO_2 has been studied as shown in figure 10b-10d. Since, adsorption of the substrate is the preliminary stage for the photocatalysis, which is more in case of nanospheres in relation to other titania nanocrystals, thus it exhibits the highest photocatalytic rate. After impregnation of Fe^{+3} and Pt^{+4} metals onto catalysts, a significant change in photocatalytic activity as compared to bare titania nanocrystals have been found for all the catalysts. This is due to the fact that impregnated metal captures the photogenerated e^- by acting as electron sink, thereby makes more availability of highly oxidative hole. However, among the Pt and Fe loaded catalysts, not much difference in their photoactivity has been found, ascribed to a small difference in their redox potential.

Several experimental results have indicated that the photocatalytic degradation rates of many organics over illuminated TiO_2 fitted the Langmuir–Hinshelwood (L–H) kinetic model. According to this model, the L–H rate form is: $r = -dC/dt = k(KC)/(1 + KC)$ where r is the initial rate of photocatalytic degradation (mol l^{-1} min^{-1}), C the concentration of the reactant after the adsorption step (mol l^{-1}), t the irradiation time (min), k the rate constant and K the Langmuir–Hinshelwood adsorption constant.

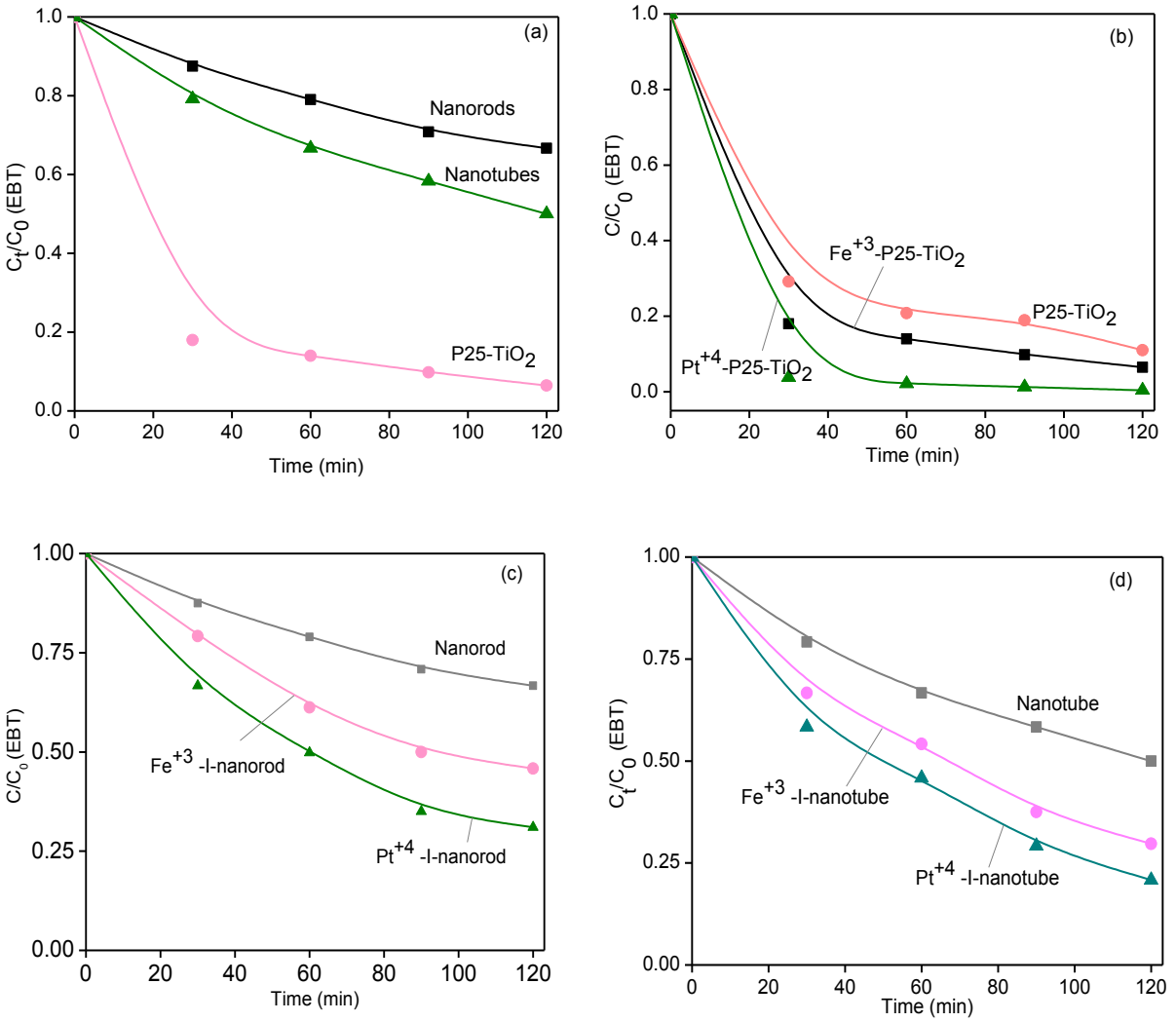

Figure 10. (a) Time course of photocatalytic degradation of Eriochrome black T by bare TiO_2 nanostructures and (b) metal loaded P25-TiO_2, (c) nanorod and (d) nanotube.

At low concentration, KC can be neglected with respect to 1 and one gets the apparent simplified equation: $r = -dC/dt = kKC$ which can be rewritten as $C/C_0 = e^{-kKt} = e^{-kt}$ where k is the apparent rate constant of the pseudo-first order (min^{-1}) reaction. In our investigation,

by plotting C/C_0 as a function of time (shown in figure 10), the concentration decreases exponentially with light irradiation time which confirms the apparent first-order kinetic law. The rate constants corresponding to these curves has been found to be 5.5×10^{-2} for P25-TiO_2, 9.04×10^{-3} for nanorods, 5.3×10^{-2} for tubes and 7.62×10^{-2} for Fe^{+3} -P25-TiO_2, etc. Thus, the photocatalytic activity was found to be improved by the metal ions loading as in Fig. 11.

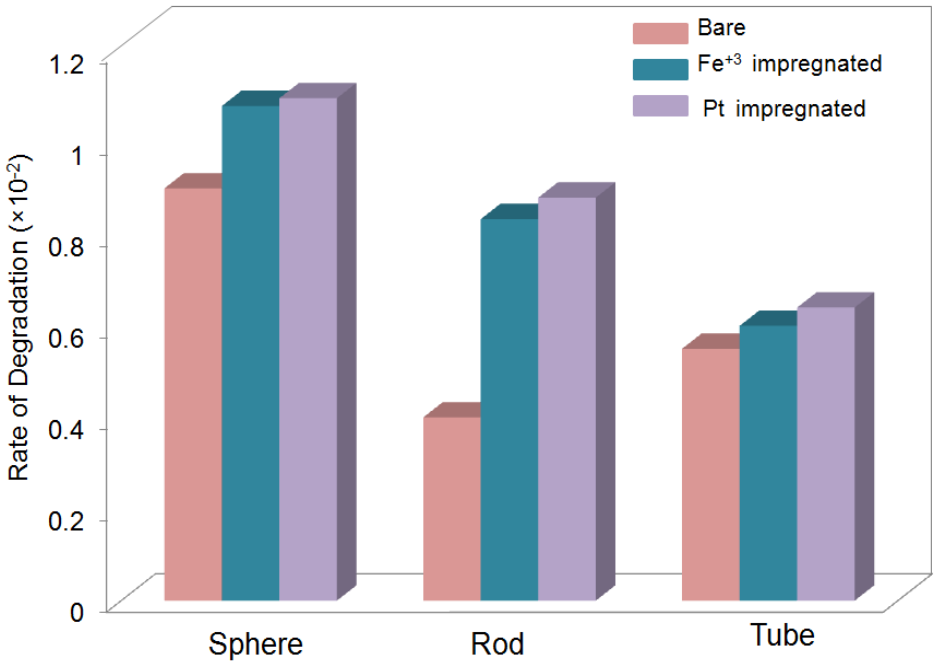

Figure 11 . Photodegradation rate of EBT as a function of TiO_2 particle shape and metal loading.

4.6. GC-MS analysis of EBT photodegradation

As the decolourisation of the EBT takes place by irradiating it under UV-light in the presence of bare and metal loaded titania nanocrystals, so in-order to determine the product of its photooxidation GC-MS analysis has been carried out (Fig. 11 and 12). It has been found that GC-chromatograph (Fig. 11a and 11c) and correspondingly mass chromatographs (Fig. 11 b and 11d) of EBT (after 2 h of irradiation) in the presence of bare and Fe^{+3}-P25-TiO_2 are almost similar, except in their respective intensities (Fig. 11a and 11c). Among the number of degraded products of EBT, four products corresponding to R_t = 7.6 (1), 8.3 (2), 10.3 (3) and 12.8 (4) min subsequent to mass chromatograph (Fig. 12) have been identified, as listed in table 2. The mechanism for the photodegradation of EBT using

titania nanocrystals is believed to take place by the photoproduced e^- and h^+, that results into formation of highly oxidative species such as hydroxal and superoxide radicals (Scheme-4), which on reaction with EBT results into its decomposition to smaller molecules.

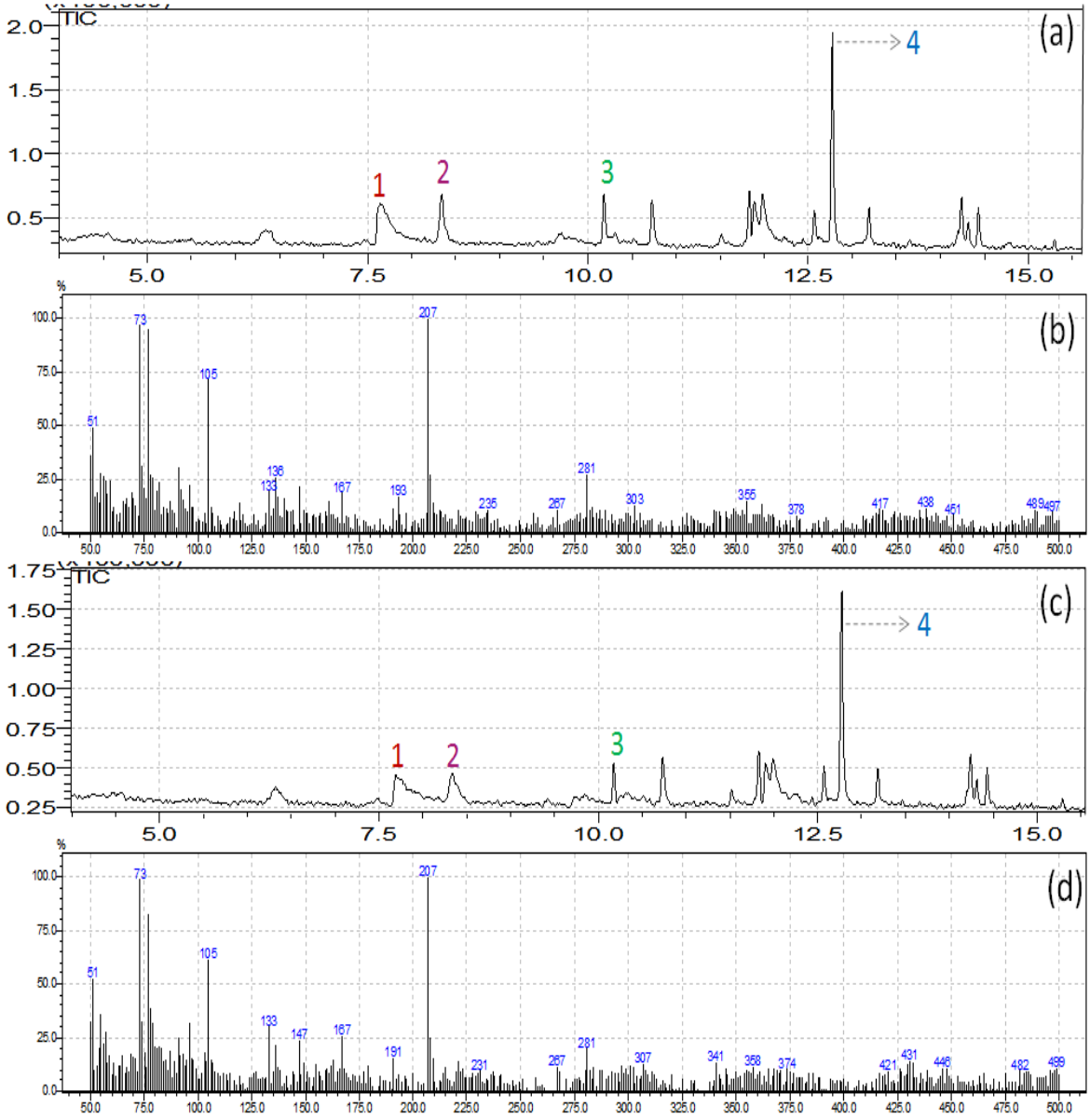

Figure 11. GC-MS spectra of EBT dye after its photodegradation for 2 h light exposure.

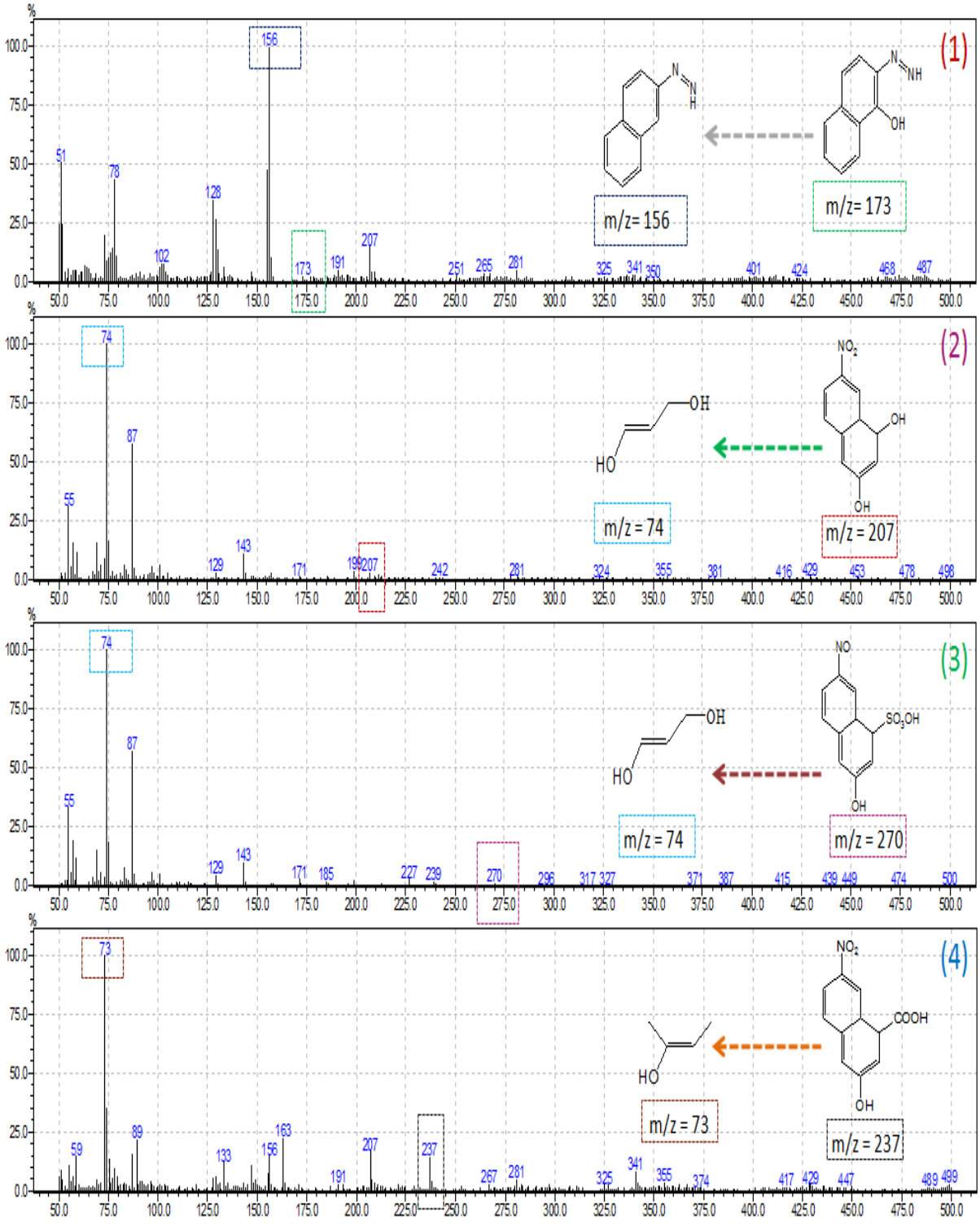

Figure 12. Mass spectra of indermediate products formed during EBT photodegradation.

Table 2: Intermediate photoproducts formed during Eriochrome black-T degradation by TiO_2 after 2h UV irradiation.

S.No	IUPAC Name of compound	Structure	MS (m/z)
1	2-diazenylnaphthalen-1-ol		173, 156, 78
2	7-nitro-1,8a-dihydronaphthalene-1,3-diol	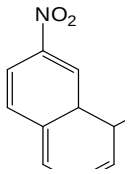	207, 87, 74
3	3-hydroxy-7-nitroso-1,8a-dihydronaphthalene-1-sulfonoperoxoic acid		270, 143, 87, 74
4	3-hydroxy-7-nitro-1,8a-dihydronaphthalene-1-carboxylic acid		237, 156, 89, 73

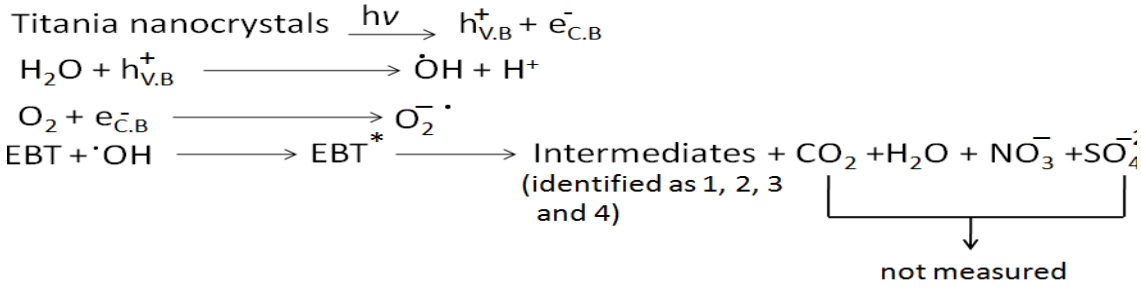

Scheme-4: Proposed mechanism for photodegradation of Eriochrome black-T dye.

5. Summary and conclusions

In summary, the influence of surface structure of TiO_2 nanostructures (P25, rods and tubes) has been evaluated (table 3) for the adsorption studies and photodegradation behavior of Eriochrome black T dye as a function of surface area, dye concentration and catalyst amount. Results showed that 20 mg catalyst of all shapes (nanospheres, nanorods and nanotubes) is the optimum amount for the 0.25 mM dye to get adsorbed completely. Despite of higher surface area for P25-TiO_2, nanorod and nanotube particles, Fe^{+3} impregnated P25 with comaparable less surface area showed enhanced adsorption rate. It is due to the presence of highly positive charge on the Fe^{+3} impregnated P25-TiO_2 results in strong attraction with anionic dye.

Table 3. Adsorption kinetics of TiO_2 nanostuctures.

			Adsorption Constant / $K_{ads} \times 10^{-2}$							
S.No	**Catalysts**		With Varying TiO_2 Concentration (mg/ml) keeping constant EBT concentration (0.25 mM)				With Varying EBT Concentration (mM) keeping constant TiO_2 concentration (4 mg/ml)			
			1	2	3	4	0.05	0.10	0.25	0.35
1.	Spheres	Bare	2.97	3.73	4.01	8.26	3.4	2.9	8.26	4.6
		Fe^{+3}	3.01	3.80	4.3	8.5	4.2	8.9	8.5	7.5
2.	Rods	Bare	0.04	1.52	1.82	2.0	2.1	2.7	2.0	5.6
3.	Tubes	Bare	1.37	2.10	2.24	3.24	1.23	2.5	3.24	3.4

The Freundlich adsorption isotherm was applied to study the extent of adsorption on various shapes of TiO_2.

Table 4. Adsorption constant and photodegradation rate constants of EBT various TiO_2 catalysts

S.NO	Catalyst	Adsorption equilibrium constant, K_{ads} μmol/mg	Rate constant, k (min^{-1}) for EBT degradation
1.	P25-TiO_2	4.8×10^{-2}	5.5×10^{-2}
2.	Nanorods	4.0×10^{-2}	9.04×10^{-3}
3.	Nanotubes	4.15×10^{-2}	5.3×10^{-2}
4.	Fe^{+3}-P25-TiO_2	5.39×10^{-2}	7.62×10^{-2}

The calculated dark adsorption equilibrium constant, K_{ads} and rate constant, k values (shown in table 4) for the EBT photodegradation under UV light exposure are found to folow the order as: Fe^{+3}-P25-TiO_2 > P25-TiO_2 > nanotubes > nanorods. Photocatalytic experiments were carried out to completely oxidized EBT dye and Fe^{+3} and Pt^{+4} impregnation led to appreciably improved the photodegradation rate.

6. References

[1] Ahmad, A. A.; Hameed, B. H. and Aziz, N., *J. Hazard. Mater.*, 2007, 141, 70-76.

[2] Barka, N.; Assabbane, A.; Nounah, A.; Laanab, L. and Ait-Ichou, Y., *Desalination*, 2009, 235, 264-275.

[3] Barka, N.; Qourzal, S.; Assabbane, A.; Nounah, A. and Ait-Ichou, Y., *J. Environ. Sci.*, 2008, 20, 1268-1272.

[4] Bavykin, D. V.; Redmond, K. E.; Nias, B. P.; Kulak, A. N. and Walsh, F. C., *Aust. J. Chem*., 2010, 63, 270-275.

[5] Dogan, M.; Alkan, M.; and Onganer, Y., *Water Air Soil Pollut*., 2000, 120, 229-248.

[6] Ferro, G. M. A.; Rivera, U. J.; Bantista, T. I.; and Moreno, C. A. C., *Langmuir*, 1998, 14, 1880-1886.

[7] Tsai, W. T.; Chang, C. Y.; Lin, M. C.; Chien, S. F.; Sun, H. F. and Hsieh, M. F., *Chemosphere*, 2001, 45, 51-58.

[8] Eren, Z.; and Acar, F. N.; *Desalination*, 2006, 194, 1-10.

[9] Robinson, T.; Chandran, P. and Nigam, P., *Water Res.*, 2002, 36, 2824-2830.

[10] Vandevivere, P. C.; Bianchi, R. and Verstraete, W. J., *Chem. Technol. Biotechnol*., 1998, 72, 289-302.

[11] Xiong, X. J.; Meng, X. J. and Zheng, T. L., *J. Hazard. Mater*., 2010, 175, 241-246.

[12] Mane, V. S.; Mall, I. D. and Srivastava, V. C., *J. Environ. Manage*., 2007, 84, 390-400.

[13] Namasivayam, C. and Kavitha, D., *Dyes and Pigments*, 2002, 54, 47-58.

[14] Namasivayam, C.; Prabha, D. and Kumutha, M., *Bioresour. Technol*., 1988, 64, 77-79.

[15] Rubin, E.; Rodriguez, P.; Herrero, R.; Cremades, J.; Barbara, I. and Vicente, M. E. S., *J. Chem. Technol. Biotechnol*., 2005, 80, 295-298.

[16] Shawabkeh, R. A. and Tutunji, M.F., *Appl. Clay Sci.*, 2003, 24, 111-120.

[17] Zaker, Y.; Hossain, M. A. and Islam, T.S.A., *Int. Res. J. Environment Sci*., 2013, 2, 1-7.

[18] Singh, A. K.; Prakash, D. and Shahi, S. K., *Int. Res. J. Environment Sci.*, 2013, 2, 25-29.

[19] Lee, S. K. and Mills, A., *J. Ind. Eng. Chem.*, 2004, 2, 173-187.

[20] Mills, A. and Lee, S. K., *J. Photochem. Photobiol. A: Chem.*, 2002, 152, 233-247.

[21] Wu, T. X.; Liu, G. M.; Zhao, J. C.; Hidaka, H. and Serpone, N., *J. Phys. Chem. B.*, 1998, 102, 5845-5851.

[22] Zhang, F. L.; Zhao, J. C.; Shen, T.; Hidaka, H.; Pelizzetti, E. and Serpone, N., *Appl. Catal.,B.*, 1998, 15, 147-156.

[23] Liu, G. M.; Wu, T. X.; Zhao, J. C.; Hidaka, H. and Serpone, N., *Environ. Sci. Technol*., 1999, 33, 2081-2087.

[24] Vinodgopal, K.; Wynkoop, D. E. and Kamat, P. V., *Environ. Sci. Technol*., 1996, 30, 1660-1666.

[25] Zhao, J. C.; Wu, T. X.; Wu, K. Q.; Oikawa, K.; Hidaka, H. and Serpone, N., *Environ. Sci.Technol*., 1998, 32, 2394-2400.

[26] Franch, M. I.; Peral, J.; Domenech, X.; Howe, R. F. and Ayllon, J., A. *Appl. Catal. B*, 2005, 55, 105-113.

[27] Bourikas, K.; Stylidi, M.; Kondarides, D. I. and Verykios, X. E., *Langmuir*, 2005, 21, 9222-9230.

[28] Chen, C. C.; Zhao, W.; Lei, P. X.; Zhao, J. C. and Serpone, N., *Chem. Eur. J*., 2004, 10, 1956-1965.

[29] Singhal, B.; Porwal, A.; Sharma, A.; Ameta, R. and Ameta, S. C., *Photochem. Photobiol. A*,1997, 108, 85-88.

[30] Han, C.; Pelaez, M.; Likodimos, V.; Kontos, A. G.; Falaras, P.; O'Shea, K. and Dionysiou, D. D., *Appl. Catal. B: Environ.*, 2011, 107, 77-87.

[31] Tang, W. Z.; Zhang, Z.; An. H.; Quintana, M. O. and Torres, D.F., *Environ. Technol.*,1997, 18, 1-12.

[32] Park, S. J. and Jang, Y. S., *J Colloid Interface Sci*., 2002, 249, 458-463.

[33] Srivastava, M. M. and Sanghi, R. (Eds.), Chemistry for green environment, Narosa Publishing House, New Delhi, 2005.

[34] Poulios, I. and Tsachpinis, I. *J. Chem. Technol. Biotechnol*. 1999, 71, 349-357.

[35] Serpone, N. and Pelizzetti, E. (Eds.), Photocatalysis: Fundamentals and Applications, Wiley, New York, 1989.

[36] Ikeda, S.; Sugiyama, N.; Pal, B.; Marci, G.; Palmisano, L.; Noguchi, H.; Uosaki, K. and Ohtani, B., *Phys. Chem. Chem. Phys.*, 2001, 3, 267-273.

[37] Fuerte, A.; Hernandez, A. M. D.; Maria, A. J.; Martinez, A. A.; Fernandez, G. M.; Conesa, J. C. and Soria, J., *Chem. Commun.*, 2001, 24, 2718-2719.

[38] Choi, W.; Termin, A. and Hoffman, M. R., *J. Phys. Chem.*, 1994, 98, 13669-13679.

[39] Rao, K. V. S.; Lavedrine, B. and Boule, P., *J. Photochem. Photobiol. A: Chem.*, 2003, 154, 189-193.

[40] Mohamed, M. M. and Al-Esaimi, M. M. *J. Mol. Catal. A: Chem.*, 2006, 255, 53-61.

[41] Grover, S. I.; Singh, S. and Pal, B., *Appl. Surf. Sci.*, 2013, 280, 366-372.

[42] Gupta, N. and Pal, B. *J. Mol. Catal. A: Chem.*, 2013, 371, 48-55.